

Oil production optimization of several wells subject to choke degradation [★]

Adriaen Verheyleweghen, Johannes Jäschke

Department of Chemical Engineering, Norwegian Univ. of Science and Technology, Trondheim, NO-7491 (e-mail: verheyle@ntnu.no, jaschke@ntnu.no).

Abstract: Unplanned maintenance interventions of subsea oil and gas production systems are very expensive, which leads to strict requirements to equipment reliability. Without a systematic way to ensure reliable operation however, a very conservative operational strategy is often chosen, which can lead to sub-optimal operation and the loss of large potential profits. We propose to integrate condition monitoring and prognostics into the production planning problem to reduce conservativeness by actively steering plant degradation and preventing violation of health-critical constraints. We achieve this by combining equipment degradation models with regular process models and solving a shrinking horizon real-time optimization problem until the next planned maintenance horizon. A network of oil and gas producing wells with artificial gas lift, subject to particle induced choke erosion is used as a case example.

Keywords: Health-aware production optimization, condition-based control

1. INTRODUCTION

In this paper we consider an oil and gas production network consisting of multiple wells. The wells are connected to a common manifold, from which the combined flow goes through a riser to a topside receiving facility. As the field matures, the reservoir pressure decreases. Eventually, the pressure might drop to such low levels that fluids can no longer overcome the resistance in the riser, and production comes to a stop. Artificial gas lift can be used to reduce the pressure drop and increase the flow, prolonging the lifetime of the field.

However, increased volume flows (and consequently velocities), in addition to the decreased density, may lead to accelerated degradation of vulnerable parts of the system. In particular, erosion of chokes and bends may be a problem, especially if the sand production from the reservoir is high. Particle erosion can severely limit the remaining useful life of exposed equipment. In rare cases, sand erosion has been known to erode away critical components such as chokes in as little as a few hours (Haugen et al., 1995). Choke replacement frequencies of 3-4 months, though having significant costs associated with them, are not unheard of in the subsea industry.

Sand production generally tends to increase as the field matures and reservoir pressure decreases, though it can also pose problems in some green fields. It is consequently vital to consider potential sand erosion when deciding on a production strategy, in order to prevent breakdowns which require costly unplanned maintenance intervention. Common industrial practice is to define an acceptable sand rate (ASR) above which operation is not permitted. The ASR is often conservatively defined in order to account

for worst-case erosion scenarios. The operational degrees of freedom for production optimization are consequently severely constrained, leading to sub-optimal operation.

The conservativeness can be reduced by monitoring the rate of erosion on critical components real time and adjusting operation to reflect equipment integrity. Monitoring usually involves periodic inspection of weight loss coupons. Real-time erosion monitoring systems, such as ABBs INSIGHT (ABB, 2010), exist, but are not yet widespread in industry. These systems are usually not integrated with the control system. Set-points of the control system must still be manually adjusted by the operator. This dependency on the operator can lead to delays, manual overrides and overall reduced efficiency of the production system.

In this paper, we use a *health-aware real-time optimization* (RTO) approach, in which health monitoring and prognostics is included in the decision making process to find the optimal operational strategy without jeopardizing equipment health (Verheyleweghen and Jäschke, 2017a). Specifically, we formulate the problem of optimal operation as a dynamic optimization problem where the objective is to maximize the overall profit of the plant, without violating constraints on the maximum allowable choke erosion. We also show how uncertainties in the model parameters can be taken into account by formulating the problem of optimal operation as a worst-case / min-max optimization problem or a multi-stage stochastic optimization problem. We implement both methods and solve the problem repeatedly in a shrinking-horizon, RTO-like fashion.

The remainder of the paper is structured as follows: In Section 2 we give a process description for the gas lifted well network. In Section 3 we formulate the optimization problem and explain how uncertainty is treated. Simulation results are presented and discussed in Section 4.

[★] We acknowledge financial support by SUBPRO center for research based innovation, www.ntnu.edu/subpro, and DNV-GL

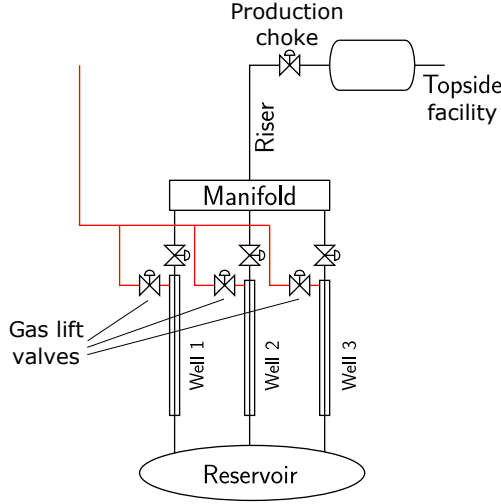


Fig. 1. Illustration of the oil and gas network with artificial gas lift.

Finally, concluding remarks are given and future work is described in Section 5.

2. PROCESS DESCRIPTION

The model for the oil and gas production system used in this work is based on the model by Krishnamoorthy et al. (2016). An illustration of the process is given in Fig. 1. A full description of the model is given there, but for the sake of completeness, we provide a summary below. The model was modified slightly in the following ways:

- (1) The model uses a larger time horizon since our aim is to do health-aware RTO, which requires the time horizon to capture the degradation dynamics. We therefore assume that changes in mass flow rates are instantaneous, resulting in constant mass hold ups. The dynamics in our work are instead dictated by gradual choke degradation and slow decline of reservoir pressure.
- (2) The model considers a three-phase system consisting of oil, gas and water.
- (3) The model is extended to include three wells and a riser

Gas injection at the bottom of the well lowers the average fluid density, thereby reducing the hydrostatic pressure drop in the well. As a result, the bottom hole pressure and consequently the flow from the reservoir increases, until a certain point. Too large gas injection rates result in increased frictional pressure drop due to increased velocities. We define the short term optimal gas injection rate (with respect to oil and gas production), as the point at which the marginal frictional pressure drop is balanced by the marginal hydrostatic pressure drop. As we shall see later, the increased velocities lead to more rapid degradation, which might force us to operate at lower-than-short-term-optimal gas injection rates.

2.1 Process model

The steady-state mass balances in each well are

$$\dot{m}_{pg} = \dot{m}_{rg} + \dot{m}_{lg} \quad (1)$$

$$\dot{m}_{pl} = \dot{m}_{rw} + \dot{m}_{ro} \quad (2)$$

$$\dot{m}_p = \dot{m}_{pg} + \dot{m}_{pl}, \quad (3)$$

where \dot{m}_{lg} is the flow rate of lift gas through the annulus, \dot{m}_{rg} is the flow rate of gas from the reservoir, and \dot{m}_{pg} and \dot{m}_{pl} are the flow rates of produced gas and liquid respectively. The liquid flow \dot{m}_{rl} is the sum of the flow of water \dot{m}_{rw} and the flow of oil \dot{m}_{ro} from the reservoir. Finally, the total flow rate through the production choke is \dot{m}_p . Adjusting the gas lift rate and the total flow through the production choke is achieved by opening and closing the valves. The flow rates can then be expressed in terms of the valve equation:

$$\dot{m}_p = C_{pc} \sqrt{\rho_w (p_{wh} - p_m)} \quad (4)$$

$$\dot{m}_{lg} = C_{lg} \sqrt{\rho_a (p_a - p_{wi})}. \quad (5)$$

Here, C_{pc} and C_{lg} are the valve coefficients of the production choke and the lift gas valve respectively, and ρ_w and ρ_a are the fluid densities in the well tubing and in the annulus. Pressures p driving the flow are denoted by wh for wellhead, m for manifold, a for annulus and wi for well injection point.

Assuming that the ideal gas law can be applied here, we express the density of the gas in the annulus as

$$\rho_a = \frac{M p_a}{T_a R} \quad (6)$$

$$= \frac{m_a}{(A_a^2 - A_w^2) L_a}, \quad (7)$$

where M is the molar mass of the lift gas, T_a is the temperature in the annulus and R is the universal gas constant. The average density in the well tubing is

$$\rho_w = \frac{m_{gt} + m_{lt} - \rho_l L_r A_r}{L_w A_w} \quad (8)$$

$$\rho_l = WC \rho_w + (1 - WC) \rho_o. \quad (9)$$

In the above expressions m_a , m_{gt} and m_{lt} are the holdups of gas in the annulus, and holdups of gas and liquid in the tubing, L_r and A_r are the length and cross-sectional area of the tubing above the gas injection point, and L_w and A_w are the length and cross-sectional area of the tubing below the gas injection point.

The flow from the reservoir is given by

$$\dot{m}_{rl} = PI \cdot (p_r - p_{bh}) \quad (10)$$

$$WC = \frac{\dot{m}_{rw}}{\dot{m}_{rl}} \quad (11)$$

$$\dot{m}_{rg} = GOR \cdot \dot{m}_{ro}, \quad (12)$$

where

$$p_r = \frac{m_{rg} RT}{V_r}. \quad (13)$$

Above, PI is the productivity index, WC is the water cut, GOR is the gas-oil-ratio, and p_r is the reservoir pressure. These are well-specific parameters.

Finally, the well pressures are decreasing as the reservoir is slowly depleting. We model the reservoir as a storage tank, yielding

$$\frac{dm_{rg}}{dt} = -\dot{m}_{rg} \quad (14)$$

2.2 Choke degradation model

Choke erosion rates depend on a number of different factors, such as physical properties of the fluid and the impacting particle. In addition, erosion rates are heavily dependent on the choke geometry, as this will influence the flow patterns. It is therefore a challenging task to predict the erosion rates for a given choke, without expensive computational fluid dynamics (CFD) simulations. DNV-GL (2015) give an overview over some erosion prediction models for simple choke geometries, based on which they recommend ASRs. We use the erosion model presented in DNV-GL (2015), which is a variation of the model presented in Haugen et al. (1995). The erosion rate is given as

$$\frac{dE}{dt} = \frac{K \cdot F(\alpha) \cdot U_p^n}{\rho_t \cdot A_t} \cdot G \cdot C_1 \cdot GF \cdot \dot{m}_{sand} \cdot C_{unit} \quad (15)$$

where $\frac{dE}{dt}$ is the erosion rate in mm/yr., K , n , C_1 , GF and C_{unit} are various constants. \dot{m}_{sand} is the sand production rate and G is defined as

$$G = \frac{d_p \cdot \beta \cdot (1.88 \cdot \log(A) - 6.04)}{D_{pipe}} \quad (16)$$

where d_p is the particle diameter, and D_p is the pipe diameter. β and A are dimensionless parameters

$$A = Re \cdot \frac{\tan(\alpha)}{\beta} \quad (17)$$

$$\beta = \frac{\rho_p}{\rho_f} \quad (18)$$

where Re is the Reynolds number of the flow, ρ_p is the particle density and ρ_f is the fluid density.

The sand production rate \dot{m}_{sand} is assumed to be proportional to the overall mass flow rate from the reservoir:

$$\dot{m}_{sand} = SR \cdot \dot{m}_r, \quad (19)$$

where SR is the sand rate parameter. Furthermore, in Equation 15, F is the ductility of the choke gallery material, which is

$$F = 0.6 \cdot [\sin(\alpha) + 7.2 (\sin(\alpha) - \sin^2(\alpha))]^{0.6} \cdot [1 - \exp(-20\alpha)] \quad (20)$$

for ductile materials. Here, α is the particle impact angle, which is given as

$$\alpha = \arctan\left(\frac{1}{\sqrt{2R}}\right), \quad (21)$$

with R being the radius of the choke gallery. U_p is the particle impact velocity, which is determined by

$$U_p = \frac{3 \cdot Q}{4 \cdot A_g} = \frac{3 \cdot Q}{8 \cdot H \cdot D}, \quad (22)$$

where Q is the actual volumetric flow rate, A_g is the effective gallery area, H is the effective height of the gallery and D is the gap between the choke cage and choke body.

3. OPTIMIZING ECONOMIC PERFORMANCE SUBJECT TO HEALTH CONSTRAINTS

By combining the process model and the health degradation model described in Section 2, the combined DAE model can be used to formulate an optimization problem in which the economic performance is maximized subject to

constraints on the maximum allowable health degradation. In previous work (Verheyleweghen and Jäschke, 2017b), we have shown that failing to include the constraints on health degradation will lead to unreliable operation, since this constraint always will be active in the optimal solution for the operation strategy.

The health state of the plant is assumed to be known at any given time, meaning that real-time erosion monitoring systems are installed and working.

The optimization problem which is solved at each RTO iteration can be written as:

$$\min_{\mathbf{u}} \int_{t_0}^{t_f} \phi(\mathbf{x}, \mathbf{z}, \mathbf{u}, \mathbf{p}) dt \quad (23a)$$

$$\text{s.t. } f(\mathbf{x}, \mathbf{z}, \mathbf{u}, \mathbf{p}) \leq 0 \quad (23b)$$

$$g(\mathbf{x}, \mathbf{z}, \mathbf{u}, \mathbf{p}) = 0 \quad (23c)$$

where ϕ is the objective function which is to be minimized, and f and g are the inequality constraints and equality constraints. The variables \mathbf{x} , \mathbf{z} and \mathbf{u} denote the differential states, algebraic states and inputs, respectively. \mathbf{p} is used to denote the uncertain parameters.

The dynamic problem (23) is discretized and solved with orthogonal collocation with three collocation points for each finite element (Biegler, 1984). The discretized problem can be written as

$$\min_{\mathbf{u}} \sum_{k=1}^N \phi(\mathbf{x}_k, \mathbf{z}_k, \mathbf{u}_k, \mathbf{p}_k) \quad (24a)$$

$$\text{s.t. } f(\mathbf{x}_k, \mathbf{z}_k, \mathbf{u}_k, \mathbf{p}_k) \leq 0 \quad \forall k = 1 \dots N \quad (24b)$$

$$g(\mathbf{x}_k, \mathbf{z}_k, \mathbf{u}_k, \mathbf{p}_k) = 0 \quad \forall k = 1 \dots N \quad (24c)$$

where N denotes the horizon length.

3.1 Uncertainty handling

To account for plant-model mismatch / parametric uncertainty, or intrinsic stochasticity of the system, we consider some of the variables (denoted \mathbf{p} in (23)) to be stochastic. In particular, it is assumed that the sand production rate SR and the productivity index PI in each of the three wells are stochastic. For simplicity, we assume that the nine uncertain variables are independent and normally distributed, $\mathbf{p}_k \sim \mathcal{N}(\mu_k, \sigma_k)$.

Various approaches for optimization under uncertainty are found in literature. Two of the most popular approaches are worst-case optimization and scenario-based optimization.

Worst-case optimization; stochasticity is acknowledged by substituting in the worst-case realizations in the uncertain parameters. If constraints are satisfied for the worst-case realization, they should also hold for other parameter realizations, for most cases. Though it can be shown that the worst-case solution may be infeasible for other parameter realizations, this approach has been successfully demonstrated for a number of practical applications.

Scenario-based optimization; in which the probability distribution of the uncertain parameters is discretized into

a finite number of scenarios and incorporated into the optimization problem in the form of a scenario tree. An illustration of a scenario with four scenarios is shown in Fig. 2.

By optimizing for all scenarios simultaneously, it is ensured that the obtained solution is not only feasible for the worst-case realization or expected realization, but for all possible realizations in the scenario tree. Furthermore, the degree of sub-optimality of the solution can be reduced by weighing the individual scenarios with their respective probabilities. This leads to a solution that is, on average, less conservative than the worst-case approach. Possibility of future recourse is included in the optimization by design of the scenario tree, which makes this method well suited to RTO problems under uncertainty.

The drawback of this method compared to the two others is the increased problem size and consequent computation time, due to the need for additional variables for each scenario.

Worst-case and scenario-based RTO maybe classified under the umbrella-term of robust optimization, in which parameter realizations are assumed to occur within bounded uncertainty sets. These approaches are perhaps the easiest to grasp conceptually, but other ways to handle uncertainty (such as chance constrained optimization, dynamic programming, and fuzzy programming) exist in literature. We will however only consider worst-case and scenario optimization in this work.

3.2 Worst-case optimization

The worst-case optimization problem can be written as

$$\min_{\mathbf{u}} \sum_{k=1}^N \phi(\mathbf{x}_k, \mathbf{z}_k, \mathbf{u}_k, \mathbf{p}_k^*) \quad (25a)$$

$$\text{s.t.} \quad \mathbf{p}_k^* = \arg \max_{\mathbf{p}_k} \|f(\mathbf{x}_k, \mathbf{z}_k, \mathbf{u}_k, \mathbf{p}_k)\| \quad \forall k = 1 \dots N \quad (25b)$$

$$g(\mathbf{x}_k, \mathbf{z}_k, \mathbf{u}_k, \mathbf{p}_k) = 0 \quad \forall k = 1 \dots N \quad (25c)$$

where \mathbf{p}_k^* is the worst-case parameter realization, i.e. the scenario which leads to the largest constraint violation. Due to the two nested optimization problems, this approach is also known as min-max optimization. These problems are generally difficult to solve or even intractable (Ben-Tal et al., 2009). In general, we must require \mathbf{p}_k to be bounded for the inner problem to have a solution. In some cases, such as the one considered in this work, the worst case parameter realization \mathbf{p}_k^* can be known a priori. This significantly simplifies the problem since the second optimization problem disappears.

3.3 Scenario-based optimization

In scenario-based optimization, we discretize the continuous distribution function into a finite number of discrete scenarios, and optimize the following objective

$$\min_{\mathbf{u}} \sum_{i=1}^S p_i \sum_{k=1}^N \phi(\mathbf{x}_{i,k}, \mathbf{z}_{i,k}, \mathbf{u}_{i,k}, \mathbf{p}_{i,k}) \quad (26a)$$

subject to the following constraints

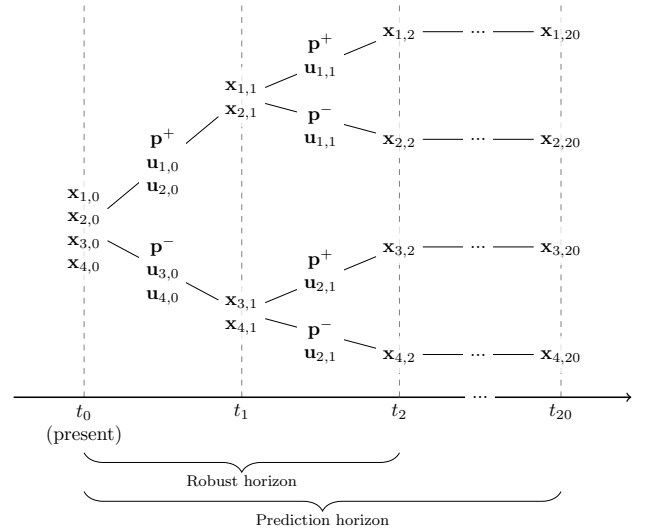


Fig. 2. Scenario tree with $N = 20$ and $S = 4$.

$$\text{s.t.} \quad f(\mathbf{x}_{i,k}, \mathbf{z}_{i,k}, \mathbf{u}_{i,k}, \mathbf{p}_{i,k}) \leq 0 \quad \forall i = 1 \dots S, k = 1 \dots N \quad (26b)$$

$$g(\mathbf{x}_{i,k}, \mathbf{z}_{i,k}, \mathbf{u}_{i,k}, \mathbf{p}_{i,k}) = 0 \quad \forall i = 1 \dots S, k = 1 \dots N \quad (26c)$$

$$\sum_{i=1}^S \mathbf{A}_{i,k} \mathbf{u}_{i,k} = 0 \quad \forall k = 1 \dots N \quad (26d)$$

where S is used to denote the number of scenarios, and p_i denotes the probability of realizing scenario i .

(26d) are the so-called non-anticipativity constraints, which are needed to enforce non-anticipativity, i.e. making sure that the optimal solution does not depend on yet unrevealed information. The scenario tree shown in Fig. 2 has $N = 20$ and $S = 4$, for example.

For the kind of scenario trees encountered in RTO problems, each branching represents the different parameter realizations due to uncertainty. One might expect that the branches from each node should be identical to the branches from its parent node. Alternatively, if the unknown parameters are estimated between each RTO iteration, this information can be included in the scenario tree by propagating the probability distribution into the future from each node and adjusting the parameter realizations of the child nodes according to the propagated probability distribution. In any case, this would lead to exponential growth of the scenario tree, with each scenario tree having n_r^N scenarios, where n_r is the number of discrete realizations of the probability distribution.

To avoid this explosive growth of scenarios, a robust-horizon $N_{robust} < N$, i.e. the stage until which branching occurs, is commonly defined (Lucia et al., 2013a). By choosing a robust horizon shorter than the RTO horizon, we disregard the possibility of future recourse, and are consequently expected to get a sub-optimal solution. However, the loss is expected to be small, since the later stages of the RTO typically do not effect the objective much. A robust horizon longer than $N_{robust} = 1$ or $N_{robust} = 2$ is rarely used, since the marginal improvement of the solution in practice rarely justifies the increased dimensionality of the

Table 1. Possible realizations considered for the uncertain parameters in the scenario-based approach.

Variable	PI , wells 1...3	SR wells 1...3
Lower	$6.3 \cdot 10^{-6}$ [-]	$0.80 \cdot 10^{-2}$ [-]
Mean	$6.5 \cdot 10^{-6}$ [-]	$0.85 \cdot 10^{-2}$ [-]
Upper	$6.7 \cdot 10^{-6}$ [-]	$0.90 \cdot 10^{-2}$ [-]

Table 2. Bound constraints

Variable	Lower bound	Upper bound	Unit
Choke opening, wells 1...3	0	1	[-]
Gas lift rate, wells 1...3	0	2.5	[kg/s]
Total gas lift rate	0	4.9	[kg/s]
Choke erosion, wells 1...3	0	0.5	[mm]

NLP. In this work, we only branch once, so $N_{robust} = 1$, which yields a two-stage stochastic program.

We further reduce the number of scenarios by limiting n_r , the number of discrete realizations used to approximate the continuous probability function. We generate the scenario tree similarly to what is proposed by Lucia et al. (2013b), i.e. by using all possible combinations of the maximum and minimum uncertain parameter realizations, in addition to a scenario for the expected and nominal uncertain parameter realizations, for a total of $n_r = S = 65$ scenarios. The possible scenario realizations are given in Table 1.

3.4 Summary of scenario-based problem formulation

The objective is to maximize the profit, i.e. maximizing the oil and gas production and minimizing the cost of produced water and the cost of gas .

$$\min_{\mathbf{x}_{i,k}, \mathbf{z}_{i,k}, \mathbf{u}_{i,k}} \sum_{i=1}^{S=65} p_i \sum_{k=1}^N NPV(\phi(\mathbf{x}_{i,k}, \mathbf{z}_{i,k}, \mathbf{u}_{i,k})) \quad (27a)$$

where

$$\phi = \sum_{well=1}^3 c_g \dot{m}_{rg} + c_o \dot{m}_{ro} + c_{lg} \dot{m}_{lg}. \quad (27b)$$

Here, NPV is the net present value with a discount factor $r = 0.1$ and c_g , c_o and c_{lg} are the gas price, oil price and gas injection cost, respectively. We assume $c_g = 3$ USD/MMBtu, $c_o = 44$ USD/bbl, $c_{lg} = 1.3$ USD/MMBtu. Bound constraints for the variables are given in Table 2. In addition come the non-anticipativity constraints and the model constraints explained in (26) for the scenario-based approach. For the worst-case method, we have that (25) and (26) are identical when $S = 1$ and the worst-case scenario \mathbf{p}_k^* is bounded and known a priori. For this particular problem, we have that the worst case scenario occurs when both PI and SR are high in all three wells.

4. RESULTS

We implemented the model in MATLAB using Casadi 3.0.0 (Andersson, 2013) and solved the NLP from the discretized problem with IPOPT (Wächter and Biegler, 2006). Both uncertainty handling strategies, i.e. worst-case RTO and scenario-based RTO, were implemented.

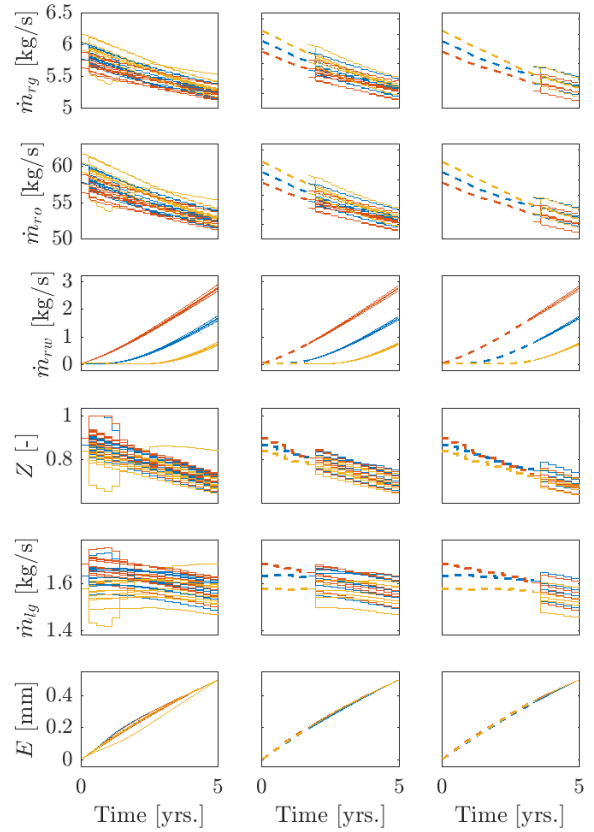


Fig. 3. Three snapshots of the open-loop solutions of the scenario-based RTO at $t = 0$, $t = 2$ and $t = 4$ years. The red, blue and yellow scenarios are for the first, second and third wells, respectively. The dashed lines show the past states, while the solid lines show the predicted states for each of the 65 scenarios.

4.1 Problem

(27) is solved repeatedly in a shrinking horizon fashion, starting with $N = 18$. After finding the optimal solution, only the first input is implemented on the actual plant, before the model is re-optimized. This process is illustrated in Figure 3, which shows the open-loop solution of the scenario-based optimization problem at three selected times $t = 0$, $t = 2$ and $t = 4$ years. The predicted states for the 65 scenarios are shown in solid lines, while past states are shown as dashed lines. It can be seen that the first inputs are identical for all scenarios due to the non-anticipativity constraints. Red, blue and yellow color distinguish the first well, second well and third well, respectively.

Figure 4 shows the closed-loop solution of the scenario-based method (solid line with circular markers) compared with the worst-case method (dotted line with cross markers). The total profit of the two operational strategies, in terms of (27a), is 6.91 bn. USD for the scenario approach and 6.75 bn. USD for the worst-case approach. Although the actual numbers should be taken with a pinch of salt, the relative difference of approx. 2.5% is significant.

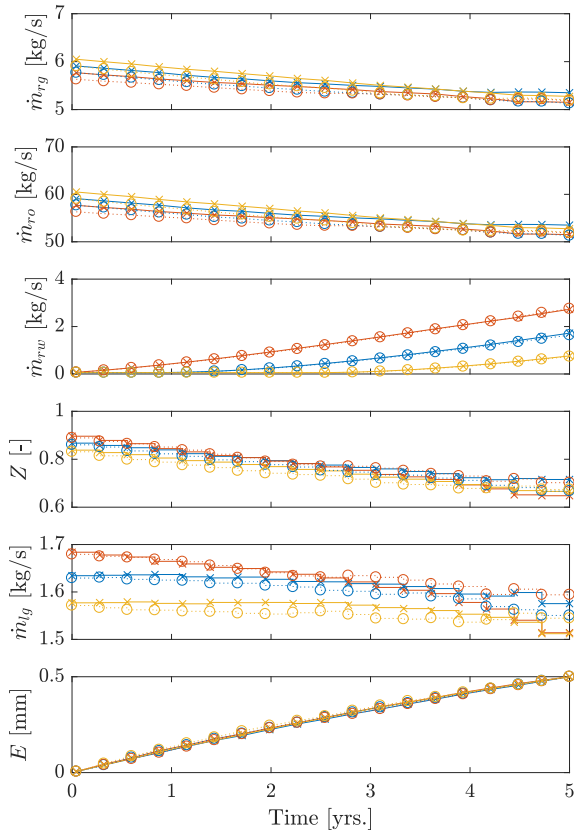


Fig. 4. Closed-loop solutions for the compared approaches. The solid line with circular markers shows the scenario-based RTO, while the dotted line with cross markers shows the worst-case RTO. The red, blue and yellow scenarios are for the first, second and third wells, respectively.

4.2 Discussion

In this work, we have assumed full state feedback, meaning that the initial values for the states are perfectly known. To simulate plant model-mismatch, the uncertain parameters are perturbed with random noise between each RTO iteration.

Since NPV of production is maximized, we see that early production is higher than late production. Due to depleting reservoir pressure, we also see the need for more lift gas as the field matures. However, due to the decreased density and consequent higher erosion rates, overall production must be throttled down to prevent choke failure, as only so much production can be permitted over the lifetime of the field.

5. CONCLUSION AND FUTURE WORK

Our health-aware RTO framework combined diagnostics, prognostics and production optimization of a subsea gas-lifted oil and gas production network subject to sand particle induced choke erosion. We show that by combining a prognostic model for the choke erosion in the production optimization, we can make sure that critical erosion levels

are not exceeded during operation, which means that the risk of costly unforeseen maintenance interventions is minimized. We also show that parametric uncertainty in the model should be handled with a scenario-based stochastic optimization approach, as this leads to better economic performance than the conservative min-max formulation that is commonly used.

The objective of the paper is to showcase the efficacy of our framework, rather than providing results which correspond 1:1 with real field data. We have therefore used a simple choke degradation model and reservoir model. It is understood that accurate models must be developed for the specific equipment in question before real-world implementation. These degradation models will have to be developed by CFD simulations and/or in collaboration with equipment manufacturers. Furthermore, future work will address the issue of overall plant reliability vs. single component reliability, as correlation between failure modes may significantly impact the overall plant reliability.

ACKNOWLEDGEMENTS

This work is funded by the SUBPRO center for research based innovation, www.ntnu.edu/subpro, and DNV-GL.

REFERENCES

- ABB (2010). Condition Monitoring and Production Optimization Insight - Erosion Management System. https://library.e.abb.com/public/a19574f541925d408525771b004ba78b/TP002_Insight_erosion_management_system.pdf.
- Andersson, J. (2013). *A General-Purpose Software Framework for Dynamic Optimization*. Ph.D. thesis, Arenberg Doctoral School, KU Leuven.
- Ben-Tal, A., El Ghaoui, L., and Nemirovski, A. (2009). *Robust Optimization*. Princeton University Press.
- Biegler, L.T. (1984). Solution of dynamic optimization problems by successive quadratic programming and orthogonal collocation. *Computers & chemical engineering*, 8(3-4), 243–247.
- DNV-GL (2015). Recommended practice RP-O501: Managing sand production and erosion. <https://rules.dnvgl.com/docs/pdf/dnvgl/RP/2015-08/DNVGL-RP-O501.pdf>.
- Haugen, K., Kvernfold, O., Ronold, A., and Sandberg, R. (1995). Sand Erosion of Wear-Resistant Materials: Erosion in Choke Valves. *Wear*, 186, 179–188.
- Krishnamoorthy, D., Foss, B., and Skogestad, S. (2016). Real-Time Optimization under Uncertainty Applied to a Gas Lifted Well Network. *Processes*, 4(4), 52.
- Lucia, S., Finkler, T., and Engell, S. (2013a). Multi-Stage Nonlinear Model Predictive Control Applied to a Semi-Batch Polymerization Reactor under Uncertainty. *Journal of Process Control*, 23(9), 1306–1319.
- Lucia, S., Subramanian, S., and Engell, S. (2013b). Non-Conservative Robust Nonlinear Model Predictive Control via Scenario Decomposition. In *Control Applications (CCA), 2013 IEEE International Conference on*, 586–591. IEEE.
- Verheyleweghen, A. and Jäschke, J. (2017a). Framework for Combined Diagnostics, Prognostics and Optimal Operation of a Subsea Gas Compression System. In *2017 IFAC World Conference*, volume 50, 15916–15921.
- Verheyleweghen, A. and Jäschke, J. (2017b). Health-Aware Operation of a Subsea Gas Compression System under Uncertainty. In *Foundations of Computer Aided Process Operations / Chemical Process Control 2017. FOCAPO/CPC*.
- Wächter, A. and Biegler, L.T. (2006). On the Implementation of an Interior-Point Filter Line-Search Algorithm for Large-Scale Nonlinear Programming. *Mathematical programming*, 106(1), 25–57.